ULTRASONIC NDT AND IMAGING OF CENTRIFUGALLY CAST STAINLESS STEEL SAMPLES

Nihat M. Bilgutay, Jafar Saniie* and Rashmi Murthy

ECE Dept., Drexel University, Philadelphia, PA 19104 and
*ECE Dept., Illinois Institute of Technology, Chicago IL 60616

INTRODUCTION

Centrifugally cast stainless steel (CCSS) components are currently being used in many critical industrial applications such as nuclear reactors, which have stringent inspection requirements. Non-destructive testing (NDT) of these components are governed by strict guidelines to insure safe operating conditions. Current literature indicates that ultrasonic NDT techniques provide potentially the most promising and reliable methods for the inspection of CCSS components. However, the received signal often has low signal-to-noise ratio (SNR) due to ultrasonic attenuation caused by grain scattering. Furthermore, ultrasonic inspection of CCSS components is plagued by high attenuation, velocity variations, mode conversion, beam divergence and/or convergence, and skewing. Therefore, the signals arising from metallurgical discontinuities or defects caused by thermal fatigue and stress corrosion, can appear to a manual ultrasonic inspector as random, stationary-noise signals. The ability to detect such defects is at best limited with the conventional non-destructive evaluation techniques. In this paper, some spectral methods are presented to improve flaw visibility by reducing the background noise from the CCSS microstructure.

In previous work, novel diversity techniques have been developed which shift either the frequency or position of the transducer to decorrelate the microstructure noise and subsequently process the resulting signatures by nonlinear signal processing algorithms to enhance flaw detection. Alternatively, a technique called "Split-Spectrum Processing" (SSP) was developed[1-2], in which a broadband signal is transmitted and the received signal spectrum is divided into a number of different frequency bands using N narrowband Gaussian bandpass filters to obtain a set of decorrelated signals as shown in Fig. 1.

The performance of the nonlinear SSP algorithms were examined in earlier work [3-6]. The SNR based on a hypothesis testing model was defined as:

$$SNR = \frac{E\{r \mid H_1\}}{\text{rms}\{r \mid H_0\}} \qquad (1)$$

where E{ } and rms denote the expected and the root-mean-square values, respectively,

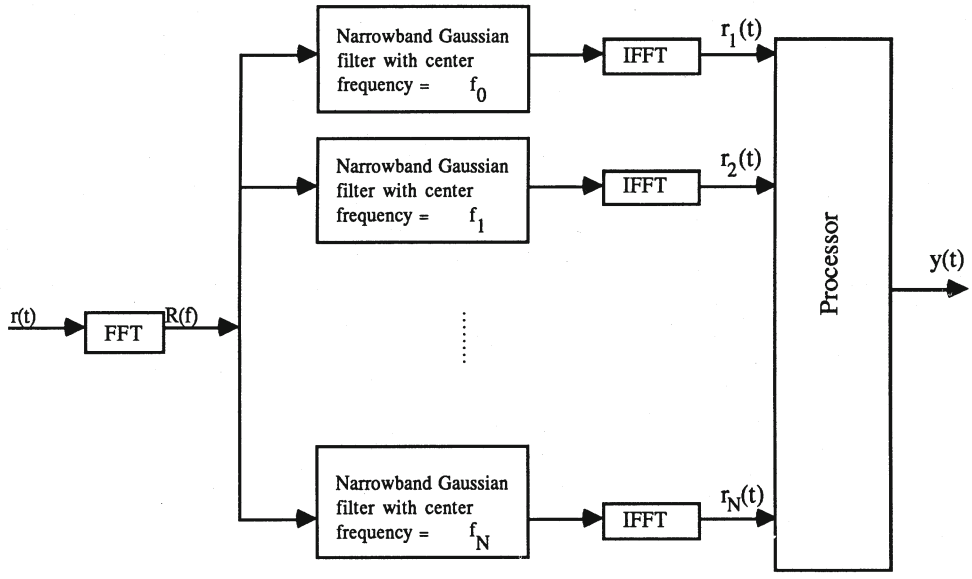

Figure 1 Block diagram of split-spectrum processing (SSP) technique

and

$$H_1: \; r = m + n \qquad \text{defect present} \qquad (2)$$
$$H_0: \; r = n \qquad \text{no defect}$$

where m is the peak value of the flaw echo and n is the zero-mean Gaussian random variable with variance σ^2, representing the grain noise component.

Polarity Thresholding (PT) Algorithm

The PT algorithm is based on the principle that at time instants where the flaw signal is present the corresponding SSP data set will not exhibit any polarity reversal since the flaw signal will dominate the grain noise (i.e., all the elements of the corresponding column will have the same polarity). However, if the data set contains only grain noise, which is zero-mean, then it is likely that the data will exhibit polarity reversal. Therefore, by setting the amplitude of the processed signal to zero at time instants where polarity reversal occurs while maintaining the original value of the unprocessed wideband signal when the data has identical polarity, the grain noise level can be reduced significantly.
Therefore, the output of the PT algorithm can be expressed as:

$$\begin{aligned} y(t) &= r(t), \quad \text{if } r_i(t) > 0 \text{ or } r_i(t) < 0, \text{ for all } i \quad \text{and} \\ &= 0, \quad \text{if sign change occurs} \end{aligned} \qquad (3)$$

The SNRE can be calculated directly from the input statistics using basic probability concepts [3,4] resulting in

$$SNRE = \frac{P_D}{(P_{FA})^{1/2}} \qquad (4)$$

where P_D and P_{FA} are the probabilities of detection and false alarm, respectively,

$$P_D = \left[\frac{1}{2} + \frac{1}{2}\,\mathrm{erf}\left(\frac{k}{\sqrt{N}}\right)\right]^N + \left[\frac{1}{2} - \frac{1}{2}\,\mathrm{erf}\left(\frac{k}{\sqrt{N}}\right)\right]^N \quad \text{and} \quad P_{FA} = 2^{(1-N)} \qquad (5)$$

Therefore, the SNRE for PT reduces to

$$(\mathrm{SNRE})|_{PT} = \frac{\left[1 + \mathrm{erf}\left(\frac{m}{\sqrt{2N}\,\sigma}\right)\right]^N + \left[1 - \mathrm{erf}\left(\frac{m}{\sqrt{2N}\,\sigma}\right)\right]^N}{2^{(N+1)/2}} \qquad (6)$$

The $\mathrm{SNRE}|_{PT}$ curves using Eq. 6 are plotted in Fig. 2 as a function of the number of windows, N, for different input SNR values (m/σ). It is evident from these curves that the performance of the PT algorithm shows sensitivity to the input SNR and the number of windows. The peak SNRE value (for a given input SNR) corresponds to the optimum choice of N, which in turn determines the optimum window bandwidth and reflects the best trade-off between probability of detection (P_D) and probability of false alarm (P_{FA}).

Another measure of performance, the receiver operating characteristic (ROC) curves are plotted in Fig.3, with input SNR as a parameter. For N = 1, which corresponds to the unprocessed signal, both the probabilities of detection and false alarm are unity. However, as N increases, the probability of false alarm is seen to decrease much more rapidly than the probability of detection especially as the input SNR decreases.

Minimization

The minimization algorithm involves choosing the minimum absolute value of the ensemble of random variables r_i for a given time instant. The output may be written as:

$$y_{MIN}(t) = \mathrm{MIN}\,\{x_i(t): i = 1, 2, \ldots N\}, \qquad (7)$$

where $x_i = |r_i|$.

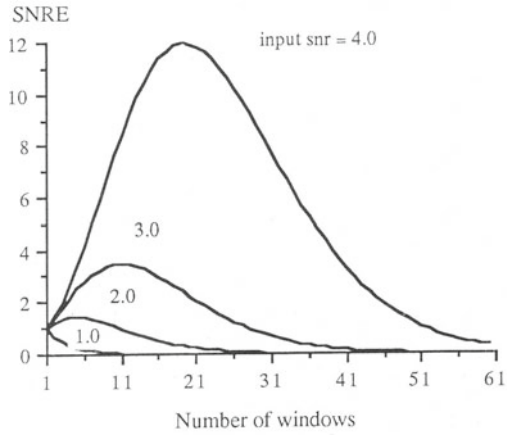

Figure 2 SNRE for PT

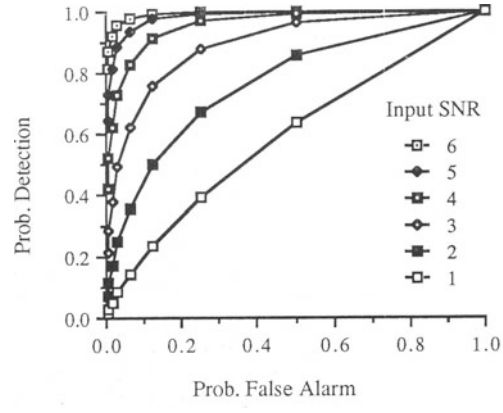

Figure 3 ROC for PT

The SNR at the output of the minimization algorithm is given by

$$(SNR)_{MIN} = \frac{E[y|H_1]}{rms[y|H_0]} = \frac{\int_0^\infty Y f_y(Y|H_1)\, dY}{\left[\int_0^\infty Y^2 f_y(Y|H_0)\, dY\right]^{1/2}} \qquad (8)$$

where Y denotes the random variable correponding to the minimization algorithm output. The SNRE curves comparing the PT and minimization algorithms were presented in earlier work [3-5] and indicates the superior performance of PT over minimization, especially as N increases.

PT-on-Minimization

This algorithm combines the advantages of the two algorithms by using the output of the minimization process when frequency diverse data exhibit no polarity reversal. Therefore, the output of this algorithm can be expressed as:

$$y(t) = y_{MIN}(t), \quad \text{if } r_i > 0 \text{ or } r_i < 0, \text{ for all } i \quad \text{and} \qquad (9)$$
$$= 0, \quad \text{if sign change occurs}$$

EXPERIMENTAL RESULTS

The algorithms described above were experimentally tested on two angle block CCSS samples each with a circular hole representing the flaw. One of the specimens is composed of equiaxial grains and the other of columnar dendritic grains. The equiaxial grain sample contains randomly distributed, fine or coarse grains with no preferential direction for wave propogation. This results in considerable variations in the wave propogation parameters depending on the local grain structure. The columnar grained sample contains columnar dendritic grains which are highly oriented, generally in the direction of the pipe radial direction. The experimental data was obtained using a 1" diameter KB-Aerotech Alpha transducer of center frequency 1 MHz in the contact mode. Data was collected from the top surface and from both the angled sides. Specimen dimensions are given in Fig. 4.

The rectified outputs for the various algorithms using both A-scan and B-scan data are presented in Figs. 5 - 7. The data shown in Fig.5 was collected from the top surface of the equiaxial grained sample, and the reflections from both the flaw and the back surface are visible. However, the processed data from all three algorithms results in nearly complete suppression of the grain echoes.

The unprocessed data in Fig. 6a was collected from side 'A' of the equiaxial grained sample. The flaw echo cannot be identified easily because of the presence of high amplitude grain noise. All the processed results in Fig. 6, however, clearly identify the flaw echo. The PT and PT-on-minimization algorithms suppress all the grain echoes, retaining only the flaw echo. Note that the back surface of the sample is not visible because of the inclined surface from which the data was obtained. Similar results were obtained for data measured from side 'B'.

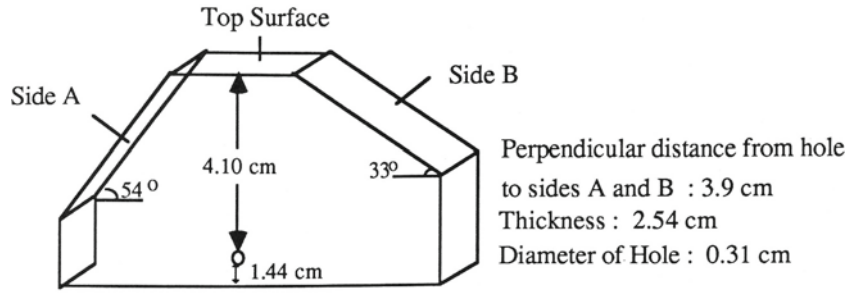

Figure 4 Diagram of the angle block specimens

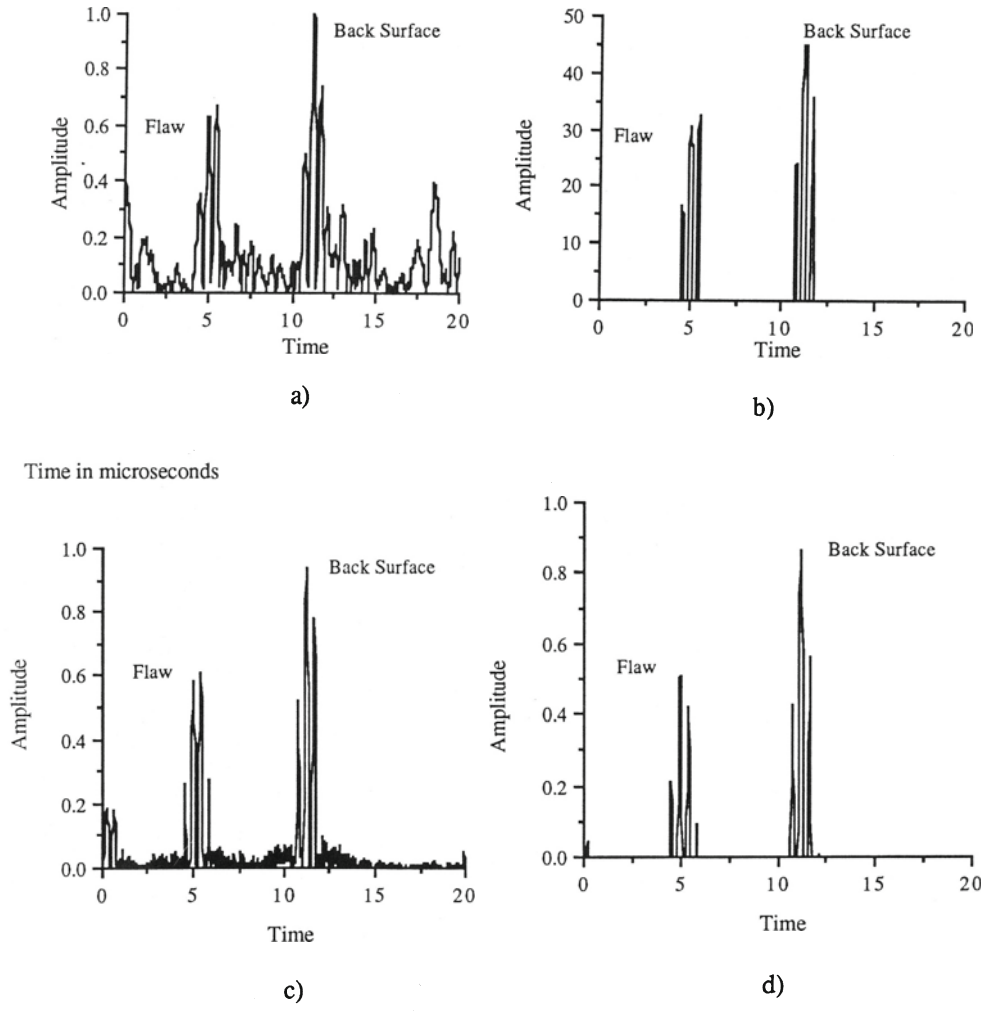

Figure 5 CCSS data for equiaxial grained sample from top surface:
(a) received signal; (b) PT; (c) minimization; (d) PT-on-minimization

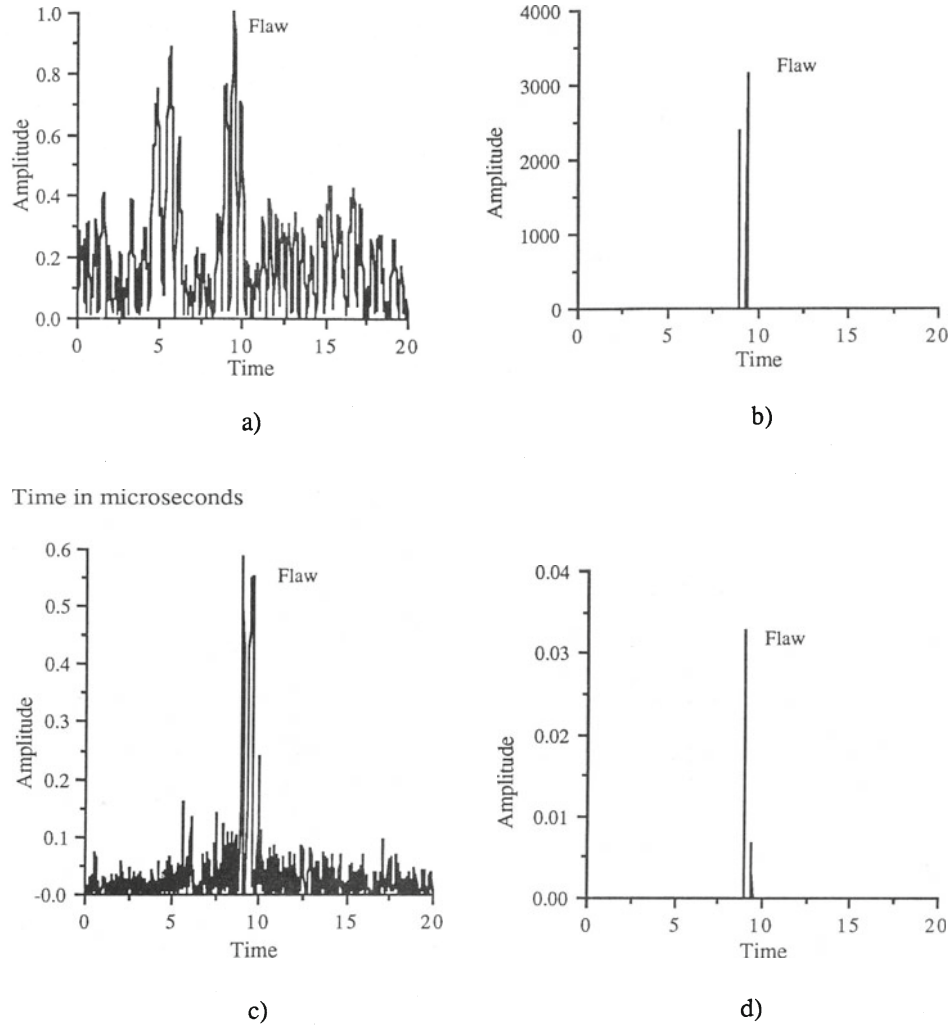

Figure 6 CCSS data for equiaxial grained sample from side 'A':
(a) received signal; (b) PT; (c) minimization; (d) PT-on-minimization

Figure 7 presents B-scan images from the top surface of the equiaxial grained sample. The images presented here are comprised of 32 equally spaced (0.4 mm) A-scans, each consisting of 650 data points obtained at a sampling frequency of 100 MHz. It should be noted that these images have relatively low resolution due to the limited transducer bandwidth (0.5 MHz) and beam spreading effects. The SSP technique was modified for B-scan imaging by using 2-D format for all operations [4,5]. The processed images result in significant grain noise suppression. A large reflection is observed in the PT images, indicating a possible defect near the front surface of the sample. Furthermore, as predicted theoretically, the PT algorithm results in superior enhancement, compared to the minimization algorithm. The performance of PT-on-minimization is similar to that of PT. These observations are also in agreement with the A-scan data presented above. The performance of the algorithms for the columnar sample was similar to the above results for the equiaxial sample, and will not be presented here due to lack of space.

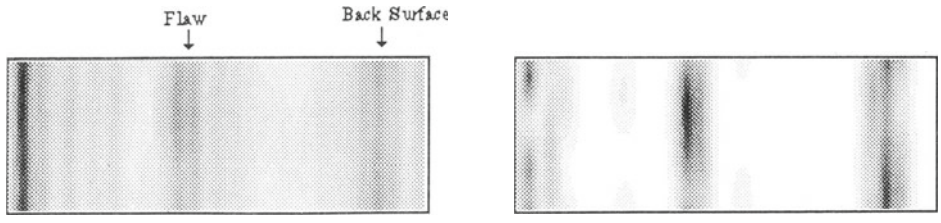

a) Unprocessed Data

b) PT

c) Minimization

d) PT on Minimization

Figure 7 2-D CCSS data for equiaxial grained sample from top surface: (a) received signal; (b) PT; (c) minimization; (d) PT-on-minimization

EVALUATION OF THE ALGORITHMS USING CCSS DATA

There are three processing parameters which basically govern the performance of the algorithms: i) spectral region over which SSP is performed, ii) window bandwidth and, iii) window spacing (i.e., the number of windows, N). Though the theoretical derivations were based on the assumption of non-overlapped windows, in experimental analysis it was found that the overlapping of adjacent windows is necessary for optimal performance. The optimal processing parameters for the SSP algorithms were obtained experimentally using A-scan data.

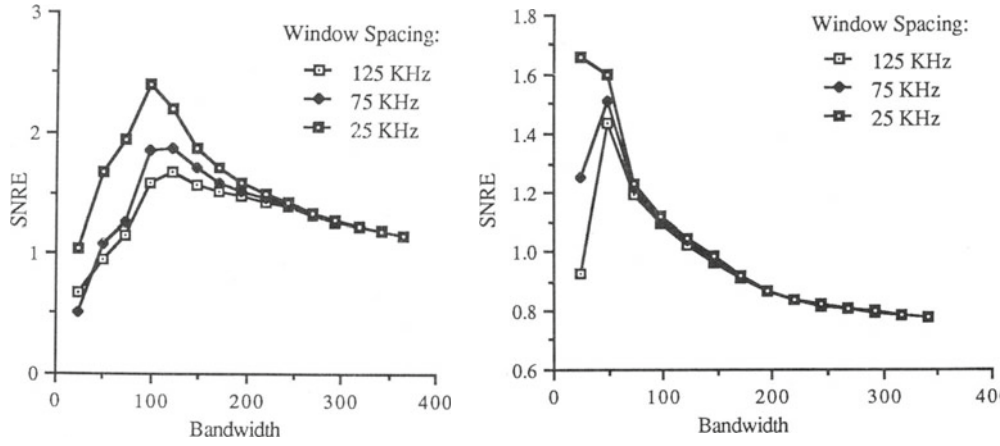

a) Minimization

b) Polarity Thresholding

Figure 8 Dependence of algorithm performance on window bandwidth and spacing (columnar grains)

The variation of SNRE with window bandwidth and spacing for PT and minimization algorithms were examined for columnar and equiaxial grain samples, yielding similar results. The results in Fig. 8 reflect the average of six independent data sets for the columnar grain sample. They indicate that the smallest window spacing, which corresponds to the FFT resolution (i.e., 25 KHz) generally provides the maximum enhancement for both types of grains. For the minimization algorithm, the optimal window bandwidth is found to be 75 and 100 KHz for the equiaxial and columnar grained samples, respectively. For the PT algorithm, the optimal window bandwidth is 25 KHz for both samples. Therefore, it is clear that the PT algorithm requires smaller window bandwidth for optimal performance compared to the minimization algorithm. Intuitively, the optimal window bandwidth must be large enough to prevent significant interference between the target and clutter echoes, which would be detrimental to performance, but not too large as to yield only minimal decorrelation of clutter echoes from different windows within the spectral range. Therefore, the optimal bandwidth value reflects a trade-off between effective clutter echo decorrelation within the available spectral range and the target echo resolution.

CONCLUSIONS

The work presented here examined the application of the SSP technique for detection of defects in CCSS samples. As expected from the theoretical SNRE derivations, the nonlinear PT and minimization algorithms were shown to provide significant enhancement in the signal-to-noise ratio. The optimal processing parameters for the two nonlinear SSP algorithms were identified experimentally, which indicate that the choice of window bandwidth and spectral region are the most critical parameters. These parameters were shown to be relatively similar for both the columnar and equiaxial samples. The bandpass filtering technique, which yielded substantial grain noise suppression in stainless steel data in previous work, was unsuccessful in providing SNRE for the CCSS samples. Therefore, the experimental results indicate that the SSP technique in conjunction with the nonlinear algorithms, is highly effective in suppressing grain noise and enhancing the flaw signal in CCSS components, which are used in many critical industrial applications.

ACKNOWLEDGEMENTS

This work was supported by EPRI Grant No. RP 2405-22.

REFERENCES

1. N.M. Bilgutay, J.Saniie, E.S. Furgason and V.L. Newhouse, "Flaw-to-Grain Echo Enhancement," Ultrasonics International-1979, pp. 152-157, May 1979.
2. V.L. Newhouse, N.M. Bilgutay, J. Saniie, and E.S. Furgason, "Flaw-to-Grain Echo Enhancement by Split-Spectrum Processing," Ultrasonics, Vol. 20, No. 2, pp.59-68, March 1982.
3. U. Bencharit, J.L. Kaufman, N.M. Bilgutay, and J.Saniie, "Frequency and Spatial Compounding Techniques for Improved Ultrasonic Imaging," Proceedings 1986 Ultrasonics Symposium, pp 1021-1026.
4. N.M. Bilgutay, U. Bencharit, and J. Saniie,"Nonlinear Spectral Processing Techniques for Ultrasonic Imaging," Review of Progress in Quantitative NDE, Vol.7-A, pp.757-767, D. Thompson and D. Chimenti, Eds., Plenum Press, New York, 1988.
5. N.M. Bilgutay, J. Saniie and U. Bencharit, "Spectral and Spatial Processing Techniques for Improved Ultrasonic Imaging of Materials", NATO ASI Series, Vol. F 44, Signal Processing and Pattern Recognition in NDE of Materials, C.H. Chen, Ed., Springer-Verlag, Berlin, 1988.
6. I. Amir,"Clutter Suppression and Texture Estimation in Non-Destructive Evaluation," Ph.D. Thesis, Drexel University, June 1986.